1   # Urban Wind: Characterization of Useful Gust and Energy Capture

2   F. C. Emejeamara, A.S. Tomlin*, J.T. Millward Hopkins

3   Energy Research Institute, School of Chemical and Process Engineering, University of Leeds, Leeds, LS2

4   9JT, UK

5   • Corresponding author, A.S.Tomlin@leed.ac.uk

6

7

8   **Abstract**

9   Small-scale wind turbine operations within the urban environment are exposed to high levels of gusts and

10   turbulence compared to flows over less rough surfaces. There is therefore a need for such systems to not

11   only cope with, but to thrive under such fluctuating flow conditions. This paper addresses the potential

12   importance of gust tracking technologies within the urban environment via the analysis of the additional

13   energy present in the gusty wind resource using high resolution measurements at two urban roof-top

14   locations. Results demonstrate significant additional energy present in the gusty wind resource at high

15   temporal resolution. This energy is usually under-represented by the use of mean wind speeds in

16   quantifying the power in the wind over longer averaging times. The results support the promise of

17   capturing a portion of this extra energy through gust tracking solutions. The sensitivity of this

18   "additional" wind energy to averaging time interval is also explored, providing useful information for the

19   design of gust tracking or dynamic control algorithms for small-scale turbines. Relationships between

20   turbulence intensity and excess energy available are drawn. Thus, an analytical model is proposed which

21   may prove useful in predicting the excess energy available across wide areas from, for example, boundary

22   layer turbulence models.

23

26

27

28   **1.   Introduction**

29   Rising uncertainties over the future of oil and gas markets and increasing awareness of anthropogenic

30   contributions to climate change have stimulated the quest for sustainable energy resources with lower

31   CO_2 emissions than traditional fossil fuel sources. In 2008, the UK government set legally binding targets

32   for achieving an 80% CO_2 reduction by 2050 compared to the 1990 baseline [1]. One attractive option for

33   helping to achieve this target is increasing the usage of small-scale, decentralised and low-carbon energy

34   sources, known as micro-generation. This would encourage energy generation close to the point of usage

35   thereby reducing transmission losses. The UK government demonstrated its commitment to micro-

36   generation with the introduction of the feed-in-tariff (FIT) system in 2010 [2]. The FIT system guarantees

37   a fixed financial return for every kWh of renewable electricity generated. Investment in micro-generation

38   has therefore become financially attractive, although only if income generated can outweigh initial

39   installation and maintenance costs over the lifetime of the installation. The efficiency of the installation

40   must therefore be optimal for the available local energy resource in order to maximise energy and

41   financial returns.

42

43   Wind energy is currently enjoying the status of a commercially proven and cost effective technology with

44   significant recent increases in annual global installed capacity [3, 4]. The expansion of this industry into

45   rural areas has occasionally been met with public disapproval. However, the smaller and quieter wind

46   energy systems that have been developed for use in urban and rural areas may be less subject to these

47   concerns. These small-scale wind turbines can easily blend into the city through either the incorporation

48   of building mounted turbines in high rise city centres, or ground mounted turbines in semi-urban regions.

49   This would lessen the losses experienced within the electricity supply system [5], as well as creating

50   greater public awareness of renewable energy options. It is estimated that the installed capacity of

51   micro/small-scale wind turbines in the UK could reach 1.3GW by 2020 [6] if appropriate incentives and

52   policies are put in place.

53

54   Urban and semi-urban wind environments are characterised by rapidly fluctuating, turbulent winds. This

55   results from various factors including high surface roughness, the interaction between incoming flows

56   and complex local building structures, and atmospheric instabilities caused by local heat sources [7]. The

57   resulting complex, gusty urban wind rapidly changes in both magnitude and direction over a range of

58   length and time-scales which may vary according to incoming wind direction and therefore upwind

59   roughness characteristics. Roughness also strongly influences mean wind speeds and the urban surface is

60   expected to slow down the mean wind close to the surface due to frictional and form drag effects [7].

61   These complex characteristics of urban wind resource have strong consequences on energy generation.

62   McIntosh *et al* [8] for example, highlighted the inability of rural-specific turbine rotor designs in tracking

63   the high fluctuations inherent in the gusty urban wind resource. However, there exists a significant

64   amount of energy stored within the higher frequency components of these gusts (as illustrated in the

65   micrometeorological region in Figure 1). Hence the possible extraction of this energy through advanced

66   turbine controls may partially offset the penalty of wind turbines operating in the reduced mean wind

67   speeds experienced close to urban surfaces.

68

69   Small-scale wind turbines fall into two major groups; Horizontal Axis Wind Turbines (HAWT) and

70   Vertical Axis Wind Turbines (VAWT). HAWT designs have been greatly developed over recent years,

71 but are not necessarily fundamentally aerodynamically superior to VAWTs [10]. Their efficiency is

72 highly dependent on wind direction (yawing). Small-scale HAWTs may suffer higher performance

73 degradation in gustier (urban) operating environments due to yaw misalignment with a cos^2 dependence

74 on the relative wind angle [11]. This can result in increased use of control power due to yaw corrections

75 in rapidly fluctuating conditions, potentially decreasing the overall efficiency of the turbine system.

76 VAWTs on the other hand have the ability to handle rapid changes in wind direction and operate at lower

77 tip speed ratios, resulting in reduced noise emissions. VAWTs therefore seem a potentially good choice

78 of configuration for the urban environment. However, they suffer from issues such narrower operating

79 ranges (e.g. higher cut-in wind speeds than HAWTS), lower peak efficiencies and low starting torques.

80 Many of these issues can be addressed through turbine controls [12, 13]. However, designing effective

81 controls relies on a detailed understanding of the nature of the available wind-resource in order to cope

82 with rapid changes in wind speed and the generation of rapid torques changes [14].

83

84 High temporal resolution monitoring of wind speeds within urban regions is not widespread, potentially

85 leading to higher levels of uncertainty in the assessment of wind turbine performance in urban areas [15].

86 Computational models of air flows over cities could potentially provide additional information on wind

87 characteristics and may have the advantage of providing wide spatial coverage compared to a limited

88 number of measurement sites [7, 16]. Hence it is of interest to determine whether outputs from such

89 models e.g. mean wind speeds and turbulence levels, could be used to assist in the prior assessment of

90 turbine performance and in turbine system design. For this reason, this study focuses on the assessment of

91 turbulence characteristics within urban areas and how measures of turbulence may be used to determine

92 how much energy is available to a well-controlled turbine.

93

94 The primary objective of the work is the characterization of typical urban wind resource based on high

95 resolution anemometer measurements at two urban roof-top locations considered as potential turbine

96 mounting sites. The additional energy resource available within high frequency gusts is quantified and is

97 linked to standard measures of turbulence such as turbulence intensity. We highlight the effect of

98 averaging time on the available wind power and demonstrate that the frequency of raw data must be well

99 matched to potential turbine response times in order to make accurate assessments of the excess energy

100 available to a particular turbine within gusts. By assessing the relationship between turbulence intensities

101 and the excess energy available within a built environment, we propose an analytical model for predicting

102 the excess energy and/or the total kinetic energy available at a potential turbine site. Section 2 introduces

103 the concepts of gust tracking and gust efficiency and their importance to turbine operation. Section 3

104 presents methods for the characterization of additional energy available within urban wind such as the

105 gust energy coefficient (GEC), and excess energy content (EEC), along with a brief description of the

106   selected urban sites for analysis and data processing methods. Section 4.1 presents results obtained from

107   the two approaches in evaluating the additional energy available at these urban sites. The effects of

108   averaging/turbine response time on potential turbine power output are discussed in Section 4.2. Here,

109   relationships are drawn between turbulence intensity and excess energy content, and an analytical model

110   for predicting EEC values within an urban environment is proposed. Finally the main conclusions are

111   presented in Section 5.

112

113   **2.   Background**

114   Gusts are defined as sudden fluctuations in wind speed which may contain within them wind speeds as

115   high as 30-50% above the average [14]. An example of the gusty nature of real world urban wind speeds

116   is illustrated in Figure 2. It is shown that the wind speed varies greatly between 0.4 ms^{-1} and 14.5 ms^{-1}

117   within a very short time period. Abrupt changes are experienced between points 1 and 2 (a jump in speed

118   from 2.7 ms^{-1} to 13.2 ms^{-1} in $\leq$ 20 s) and points 3 and 4 (a jump from 2.8 ms^{-1} to 14.5 ms^{-1} in $\leq$ 40s).

119   These sudden rises and drops in wind speed, contrast with observations from coastal/open sea terrain [17]

120   or rural terrain [18]. They result from increased turbulent drag caused by the high terrain roughness

121   present within urban environments [19], rapid changes in flow direction around buildings/structures, and

122   the formation of vortices [20] leading to regions of both flow acceleration and stagnation. These vortices

123   can be influenced by various factors ranging from the effect of building area density to the substantial

124   influence of roof heights and shapes on the flow structure within the urban environment [21]. All else

125   being equal, Bertenyi *et al* [22] suggest that a turbine system could experience a 60% loss or gain in

126   power generation if relocated from a coastal/open sea site to an urban environment**.**

127

128   Thus, it is important that controls utilised within turbines to be sited within the urban environment allow

129   gust tracking which ensures that the system not only copes with, but thrives in this complex urban wind

130   resource. The aim of these technologies is to try to maintain the turbine operation within its region of

131   peak aerodynamic efficiency [22] and thus to maximise energy extraction as wind speeds fluctuate. The

132   efficiency of a wind system is commonly characterised by its power coefficient [3, 23, 24] and is given

133   as:

$$C_p = \frac{P_T}{P}, \qquad\qquad (1)$$

134   where P is the available wind power and P_T is the power generated by the wind turbine system.

135

136   Figure 3 presents a power coefficient (C_p) curve for the vertical axis QR5 wind turbine model as a

137   function of non-dimensional tip speed ratio λ, as measured in a full-scale wind tunnel test by Quiet

138   Revolution [25]. λ is defined as the ratio between the rotational speed of the tip of the turbine blade and

139   the actual velocity of the wind [26]. Although the power curve shown in Figure 3 is defined for steady

140   flow conditions, the shape of performance curves in unsteady winds has been shown to be similar [8].

141   Hence the figure serves to illustrate the region of tip speed ratios at which maximum aerodynamic

142   efficiency and therefore peak power can be achieved. Under real world gusts, it is quite possible for the

143   turbine to move from operating at point 1 (peak power) to points 2, 3 or 4 over short time-scales

144   (seconds) if the rotational speed of the turbine is not adjusted.

145

146   For better performance in a gusty wind resource, the turbine's rotational speed needs to be constantly and

147   precisely adjusted in order to enable the turbine system to operate at its peak aerodynamic efficiency (as

148   shown by C_{pmax} in Figure 3). Failure to do so could result in a significant loss in aerodynamic power,

149   especially in situations where the turbine experiences a large gust and its tip speed ratio falls into the

150   region of deep stall [8]. Here, the energy losses and low aerodynamic torque experienced may not be

151   sufficient to allow acceleration back to the turbine's correct speed. Tracking such gusts and avoiding

152   deep stall involves specific design considerations. These include low turbine inertia, real-time operating

153   conditions (as in the case of feedback controls), and a power electronics architecture which allows for

154   active control [27].

155

156   While studying flow across buildings/structures in urban environments, Cook [28] observed structure-

157   generated turbulence which resulted in the power spectral density containing an additional peak at higher

158   frequency (i.e. ≥ 0.1 Hz) than typical boundary layer turbulence. The scale of this peak was influenced by

159   the size and shape of inherent urban structures and the frequency range of its fluctuations varied across

160   different sites. Ideally, gust tracking designs would be able to capture all the power contained within this

161   additional peak up to very high frequencies. However, cost limitations may prevent the design of turbines

162   and control architectures which are able to capture this full range of frequencies. In addition, where wind

163   data is used as input to feedback control models it is usually filtered to remove fast transients which could

164   de-stabilise the selected control model (e.g. simple proportional control [8]). It is therefore of interest to

165   consider different cut-off frequencies which may represent different levels of turbine responsiveness and

166   to evaluate the extent of excess energy which may be captured for the different cut-offs. The upper limit

167   of the frequency range (cut-off frequency F_C) selected is represented in this paper as the gust frequency

168   (F_G).

169

170   The simplest and most popular method of cut-off frequency selection is made by using a low pass filter to

171   extract the lowest frequency components of the wind input. This represents the gust frequency at which

172   the maximum amount of filtering retains a targeted percentage of the power content in the turbulent wind

173 within a given period. The targeted power content percentage tends to vary with different small-scale

174 wind turbine manufacturers as a result of their different design objectives (e.g. 99% below $F_C \approx 0.1$ Hz

175 [8], 98% below $F_C \approx 0.5$ Hz [29]). The selection of different cut-off frequencies tends to affect the

176 performance of the controller as well as the turbine output variables. However, the choice of employing a

177 wind turbine system with little or no gust tracking control within the urban environment would entail the

178 system operating at a much lower F_C. This results from the system's time lag which depends on the

179 turbine inertia, controller and aerodynamic response.

180

181 The cut-off frequency has been used in this paper to define the characteristic gust frequency, with F_C

182 employed in averaging the wind input data. A snap shot of the effects of filtering data was shown in

183 Figure 2 with an F_C of 0.1 Hz. The averaging time duration ($T_C = 1/F_C$) is an important factor in gust

184 tracking, with the influence of short fluctuations on the turbine operation of a given turbine dependent on

185 the magnitude of the T_C used in averaging the incoming wind speed, turbine RPM and power. T_C

186 therefore varies with different turbine sizes and control models. The analysis of turbulence data at the

187 potential mounting site therefore needs to reflect these characteristics if the excess energy available is to

188 be properly assessed. Various turbine control techniques have been addressed in literature with the

189 optimum power/torque tracking technique a popular control strategy in achieving optimum power

190 generation [30]. For most control techniques, to run the turbine optimally requires obtaining the $C_p - \lambda$

191 dependency of the specific turbine and/or the wind speed in calculating the desired rotor speed needed to

192 vary the generator speed [31]. The difficulty and high cost of accurate measurement of urban wind and

193 the uncertainties surrounding the application of the turbine manufacturer's $C_p - \lambda$ curve at different

194 turbine sites give rise to errors which will strongly influence the turbine controls. Maximum power point

195 tracking (MPPT) algorithms have been employed in various ways to circumvent these errors but will add

196 to the overall cost of the system [32-34]. In order to evaluate the performance of VAWTs in unsteady

197 winds and the cost effectiveness of control methods, the total energy available to the turbine needs to be

198 estimated and it is here that the current work is focussed.

199

200 **3.   Methodology and Data Processing**

201 Whilst there are a number of sources of UK wind resource information available with varying degrees of

202 resolution (e.g. that available from the UK Met Office [35]), high frequency datasets for urban

203 environments (cities, towns, etc.) are much scarcer since data sets acquired for weather forecasting

204 purposes tend to be sited as far as possible in regions of uninterrupted flows. Freely available sources of

205 wind resource data such as the Numerical Objective Analysis of Boundary Layer (NOABL) database

206 contain wind speeds that do not account for the influence of the urban area upon the wind and in general

207 tend to represent long term mean wind speeds [36]. Given the complex nature of the urban wind resource,

208   for a more effective urban wind assessment, specific high resolution measured wind data are required at

209   above roof heights which may be typical of roof-top mounted turbines. Limited research data sets are

210   available for this purpose and based on the availability of data, two sites were selected for this study. The

211   first is on the roof of the Houldsworth Building at the University of Leeds, and the second is that of the

212   Whitworth Meteorological Observatory of the University of Manchester (both within the United

213   Kingdom). The areas around both of these sites are densely populated and characterized by a large

214   number of buildings and structures. Nevertheless, both of these sites well exceed the local mean building

215   heights (11.9m for Leeds and 14.2m for Manchester based on a 250 x 250 m average) and therefore could

216   be considered as possible turbine mounting locations [37].

217

218   *3.1   Site description and instrumentation*

219   *3.1.1   University of Leeds, Houldsworth Building*

220   The first wind dataset was collected at a location within the University of Leeds Campus (in this paper

221   referred to as Unileeds), Leeds, UK. This data was captured at a sampling frequency of 10 Hz using two

222   sonic anemometers (Research-Grade Gill Scientific Instruments model R3-50) located at two different

223   mast heights of 6 m and 10 m, on the top of the Houldsworth building (roof height approximately 24 m;

224   Latitude: 53.809963°, Longitude: -1.5574005°). In the results section, height 1 (H1) at the Unileeds

225   site represents data collected at mast height of 10 m, whilst height 2 (H2) represents data collected at a

226   mast height of 6 m above the roof top.

227

228   *3.1.2   Whitworth Meteorological Observatory, Manchester*

229   The second wind data set was obtained from a sonic anemometer (Gill Windmaster Pro Sonic

230   Anemometer) at a sampling frequency of 20 Hz. This was mounted on a 5 m mast located on the roof-top

231   of the George Kenyon building on the University of Manchester South campus (also known as the

232   Whitworth Meteorological Observatory site with a building height of 49 m; Latitude: 53.467371°,

233   Longitude: -2.232006°). The wind data obtained for this study was averaged at a sampling frequency of

234   1 Hz.

235

236   *3.2   Scope of data collected and analysis*

237   The wind data used within this study were collected at the respective sites between the years 2009 and

238   2011, with a year-long dataset for each site selected for analysis within this paper. It should be pointed

239   out that these are not entirely overlapping due to gaps within the available datasets. The quoted resolution

240   of the Gill sonics is 0.01 ms^{-1} with accuracies of <1.5%. Quality assurance of the data, involving the

241   handling of data outliers, was carried out within previous studies and a description of this process can be

242 found in Balogun et al. [38]. The mean wind direction (θ) and longitudinal free-stream wind speed (V)
243 upstream of the rotor are derived from the horizontal wind components, u (x-direction) and v (y-direction)
244 as follows:

$$\theta = \tan^{-1}(v/u) , \qquad (2)$$

$$V = u \cos \theta + v \sin \theta , \qquad (3)$$

247 while the standard deviation of the longitudinal wind speed is given as

$$\sigma = \sqrt{\frac{1}{T} \sum_{i=1}^{T} (V_i - \bar{V})^2} , \qquad (4)$$

248 where $\bar{V}$ is the mean wind speed, and T defines the sample time period.

249

250 The high resolution wind data, collected from each sonic anemometer, was averaged at a sample
251 frequency of 1 Hz where necessary in order to remove the very fast transients and parsed into contiguous
252 10 minute bursts, which is consistent with wind energy industry certification standards [39].

253

254 In a turbine system, the longitudinal wind speed is directed along the hub, while in characterising the
255 degree of turbulence in a burst, the standard parameter of Turbulence Intensity ($T.I.$) is employed [40].
256 This is defined as the standard deviation of the fluctuating components of the wind speed normalised by
257 the mean wind speed for over the chosen averaging period:

$$T.I. (\%) = \frac{\sigma}{\bar{V}} \times 100\% .$$

258 $$\qquad (4)$$

259 Since $T.I.$ is sensitive to the averaging period, it should only be compared for equivalent burst durations.
260 The average power available in the wind is calculated by:

$$P = \frac{1}{2} \rho A \bar{V}^3 , \qquad (5)$$

262 where ρ is the air density and A is the cross sectional area in which the air is flowing through. However,
263 there may exist additional energy within shorter frequencies in gusty conditions (as shown in Figure 1),
264 which is usually lost (or under-reported) due to the use of the mean wind velocity measurements in
265 calculating the wind power over a given period. This additional energy can be defined by two parameters;
266 the Gust Energy Coefficient (GEC) [22] and the Excess Energy Content (EEC). The GEC is defined as the
267 ratio of the integral energy inherent in the wind over a given period of time to the assumed energy by only
268 considering the mean of the wind speed within the same period:

$$GEC = \frac{\int_0^T V^3 \, dt}{\bar{V}^3 . T} .$$

269   (6)

270 The EEC, which is closely related to the GEC, is defined as the excess energy (expressed as a percentage

271 of the total integral energy) contained within transient fluctuation about the mean over a given burst

272 period:

$$EEC(\%) = (GEC - 1) \times 100\%. \qquad (7)$$

274 The values of GEC and EEC are sensitive to the length of the burst periods chosen in this paper to be 10-

275 mins in length (i.e. T = 10 mins). This is based on the fact that a spectral "gap" appears around this

276 frequency as illustrated in Figure 1, and is consistent with industry-based standard approaches for

277 certification [39].

278

279 *3.3   Assumptions*

280 The effect of wind direction on the turbine (VAWT) performance within an urban environment was

281 assumed to be negligible [27]. It is also assumed that in an idealised steady wind environment, the GEC

282 and EEC would be 1.0 and 0% respectively [22]. This indicates that the total integral energy within the

283 sample time period is reflected by the energy derived by employing the mean wind speed within the same

284 sample time period.

285

286 **4.   Results and Discussion**

287 *4.1   Effect of $T.I.$ on power and EEC*

288 Since $T.I.$ is a more commonly presented statistic describing the level of turbulence in urban areas, it is

289 first interesting to evaluate whether a relationship exists between $T.I.$ and available excess energy. The

290 monthly average wind speed values for the two sites analysed are shown in the bottom pane of Figure 4.

291 The minimum monthly average wind speed value of 2.1 ms^{-1} was observed in December, while the

292 maximum monthly average wind speed value of 5 ms^{-1} was observed in May, both at the Manchester site.

293 The yearly average wind speeds were found to be 3.3 ms^{-1}, 2.8 ms^{-1} and 3.5 ms^{-1} at the Unileeds (H1 and

294 H2) and Manchester sites respectively, with the longer term (5years) average values being somewhat

295 higher at 3.74 ms^{-1}, 3.15 ms^{-1} and 3.66 ms^{-1} at each site respectively. Therefore, the sites used in this

296 paper can be considered to possess a low to medium quality wind potential. In the top pane of Figure 4,

297 two methods of calculating the power density are shown. The dashed lines correspond to the use of 10

298 minute averages of wind speeds for the power calculations and the solid lines correspond to the average

299 power calculations at 1 s intervals. The solid line therefore represents the maximum power available if all

300 the energy in the high frequency gusts was to be captured by the turbine. There is clearly a marked

301 difference between these two methods, particularly for the Manchester site which exhibits the highest

302 turbulence intensities for most of the year. Of the two Leeds sites, H2 was shown to exhibit higher

303   turbulence intensities, which is perhaps expected since this mast height is closer to the roof than H1. In

304   addition to generally higher turbulence intensities, higher average wind power is also observed all year

305   round at the Manchester site (excluding the months of November and December) mostly likely due to the

306   fact that it is a tall building (49 m) compared to the local mean building height (14.2 m). If the additional

307   energy in the high frequency gusts was able to be captured at this type of site, it may become viable for

308   turbine siting. In section 4.2, we assess how much of this energy may be captured for different turbine

309   response times as represented by T_C.

310

311   Based on the assertion that the output variables of a VAWT are not affected by rapid changes in wind

312   direction typical of an urban environment [27], it is relevant to investigate the degree to which the power

313   output is influenced by $T.I.$ at the sites analysed. Methods for estimating the potential energy capture at a

314   specific site by incorporating a measure of turbulence (e.g. $T.I.$) are used by some experts within the wind

315   industry [41]. In addition, $T.I.$ is likely to be a model output when using, for example, computational

316   fluid dynamics, CFD [42, 43] to investigate potential turbine sites. It is therefore useful to investigate how

317   excess energy varies with $T.I.$ thus facilitating the use of such CFD models in the design of gust tracking

318   solutions.

319

320   A measure of the influence of $T.I.$ can be highlighted by binning the wind power curve according to

321   different turbulence intensity bands, as shown in Figure 5. This is a common approach employed by most

322   practitioners within the wind industry and provides relevant information as to the turbulence level at

323   which maximum power is observed and beyond which a decline is noticed in the power curve. It is

324   important to note that power curves produced by identical turbines at different sites may lead to different

325   results due to their strong dependence on the local $T.I.$ distribution, thereby making measured power

326   curves limited in terms of being comparable and transferrable [44].

327

328   Figure 5 highlights this point, by first showing how different the calculated power curves can be

329   depending on whether 1 s or 10 minute averages in wind speed are assumed. Also shown is the increase

330   in power (at 1 s) with increasing $T.I.$ at both sites with a net reduction in power experienced below $T.I.$

331   values of 50% at Unileeds (H1 and H2) and Manchester respectively compared to the average power

332   available over all frequencies. The monotonic increase in power with increasing $T.I.$ bands suggests the

333   potential of the turbine extracting at least a portion of the additional energy observed within these gusty

334   wind resource sites. Implementing fast response controls however, will entail additional capital costs, and

335   hence the level of turbulence experienced at proposed installation sites may give useful information for

336   appropriate turbine design by answering the question: how much excess energy is there worth capturing?

337

338

339   Figure 6 shows frequency plots for each site for different bins relating to $T.I.$ It therefore provides

340   relevant information as to the level to which enhanced energy extraction is required within both sites. At

341   the selected sites, the $T.I.$ is almost never less than 10% and is most frequently between 30-40%. A

342   turbine which was able to effectively capture the high frequency energy under such conditions would be

343   able to access an average of over 30% more power than would be estimated using the mean wind speed

344   alone under these conditions as suggested in Table 1. For coastal, open country and rural sites where $T.I.$

345   is more frequently below 20% [22, 45], the average additional excess energy would be much lower (of the

346   order of 10%).

347

348   In a different approach, the EEC, as defined in Section 3.2, quantifies the "excess" energy present in the

349   gusty wind resource. Results from both sites show a yearly average additional energy of 35.3%, 50% and

350   53.4% at the Unileeds (H1 and H2) and Manchester sites respectively, for a response time of 1 s. An

351   illustration of the EEC at the two sites for a year's wind input is shown in Figure 7 and Figure 8, with

352   Unileeds (H2) and the Manchester sites showing significantly higher values of EEC. These sites are 6 and

353   5 m above the roof respectively compared to 10 m for H1, and both sites showed higher $T.I.$ values

354   throughout the year than H1 (see Figure 4). Figure 8 shows a strong dependence of excess energy on wind

355   speeds as seen in previous studies [22]. A summary of the mean value of EEC at various sites from both

356   previous and the present studies, categorised according to different levels of terrain roughness, is shown

357   in Table 2. The low turbulence sites (i.e. coastal sites) suggest a minor margin of 3.3% of excess energy

358   while the high turbulence sites (i.e. urban environments) suggest a significant margin of above 23% of

359   excess energy available. What is clear from the current work is that in addition to the local roughness

360   parameters, for roof mounted sites it is also important to consider the height above roof when estimating

361   excess energy available.

362

363   Thus, from the results presented so far in Section 4.1, the two approaches used in evaluating the available

364   "excess" energy at both sites highlight the presence of a sizeable quantity of additional energy in the

365   gusty urban wind. This could assuage the uncertainties involved in urban wind assessment as well as

366   encouraging gust tracking solutions.

367

368   *4.2   Effect of T_C on Power and EEC*

369   The average wind speed across the two sites in a year was observed to be greater than 3.1 ms^{-1} and the

370   potential maximum cut off frequency (F_C) likely to be less than 1 Hz (corresponding to the maximum

371   resolvable response frequency of the turbine). Thus, dimensional reasoning, as shown in Equation 9,

372   dictates that the minimum length scale (L_u) corresponding to the characteristic maximum gust frequency

373   (F_G) employed in this study is approximately larger in magnitude than the diameter of a small-scale

374   VAWT turbine (e.g. the QR5 with diameter – 3.1 m [27]).

375

$$L_u = \frac{\bar{V}}{F_c} > D_T \qquad\qquad (8)$$

376   where D_T is the diameter of the turbine.

377

378   This means that frequencies, F_C, and/or their corresponding averaging time-scales, T_C, should be less than

379   1 Hz to be physically resolvable by the turbine. The estimated small-scale wind energy capture for an

380   urban site through a turbine will depend on the turbulence characteristics of the site (measured by $T.I.$)

381   and the response characteristics of the turbine system. T_C characterises the turbine delay in response due

382   to the difference in inertia of the turbine blades and generator (which will depend on turbine size and

383   weight) and the control system architecture [46]. Therefore a range of possible values for T_C could be

384   present for different systems. We present here two case studies and their effects on average available

385   power and EEC.

386

387   **Case 1 (Tb1)**: For the first case, the T_C employed ($T_C = 10$ s) corresponds to the shortest averaging time

388   for anticipated small-scale VAWT response characteristics as suggested in [46].

389

390   **Case 2 (Tb2)**: Case 2 represents a VAWT with a much higher system response time ($T_C = 60$ s), where

391      $F_C << F_G$. This corresponds to the averaging time used in measuring and subsequent data analysis for

392   wind turbines with rotor diameter less than 16m as described in the relevant standard, IEC $61400 – 12 – 1$

393   (see Annex H of IEC $61400 – 12 – 1$ [39])**.**

394

395   With the 10 s and 60 s averaging imposed at the two sites we examine the loss in average power and EEC

396   compared to a maximum response frequency of 1Hz, as shown in Figure 9. Tb1 and Tb2 experience a

397   lower average power loss at Unileeds (H1) as compared to other sites. This may be as a result of reduced

398   blockage and wake effects at the mast height of 10 m above roof at the Unileeds site, and the relatively

399   lower turbulence levels compared to sites nearer the roof (see Figure 4). At Unileeds (H1), Figure 9

400   suggests that Tb1 would experience a maximum loss of approximately 6.93% of the available average

401   wind power while Tb2 would experience a maximum power loss of 17.85%. Therefore, the probable

402   increase in cost of a faster responding control system may be easily offset by its potential to capture more

403   energy available in the gusts. A summary of the percentage gain in power available to Tb1 and Tb2 is

404   shown in Table 2. Regarding the EEC available at both sites, Figure 9 shows that increasing T_C tends to

405   reduce the possible additional energy available, with gust tracking solutions expected to have relatively

406   greater impact at lower mast heights, where $T.I.$ levels are likely to be higher.

407 The turbulence spectrum and the location of the turbulent energy peaks will be site dependent and hence

408 large differences may be observed with the use of different time-resolution of the data (T_C) when

409 calculating $T.I.$ at a given site. In addition, when trying to relate the excess energy that may be available

410 to a specific turbine, the use of an appropriate value of T_C is required in order to reflect the potential

411 response time of the turbine. Figure 10 demonstrates the impact of increasing T_C on average power, EEC

412 and $T.I.$ at the Manchester site (in this case, $T_C \approx 1/F_C$). Increasing T_C results in decreasing $T.I.$ and

413 decreasing average power and EEC, and vice versa. It is therefore interesting to explore whether, if

414 appropriate averaging times are chosen whether a strong relationship exists between $T.I.$ and EEC.

415 Such a relationship is demonstrated in Figure 11 where EEC is plotted against the equivalent binned

416 values of $T.I.$ for several values of T_C. The figure shows that all the data lie close to a best fit curve which

417 was determined to be a cubic function using a least squares error approach within MATLAB's best fit

418 tool. Thus, EEC values were approximated by an empirical relationship given by the following equation:

419
$$EEC = 0.00022 T.I.^3 + 0.019 T.I.^2 + 0.15 T.I. -0.38 \qquad (9)$$

420

421 with a correlation coefficient value (R^2) of 0.9986. The coefficient was calculated based on the EEC

422 values from site observations (as shown in Fig. 11), using MATLAB's fitting tool. The high correlation

423 coefficient value (R^2) indicates a good agreement between EEC values from site observations and

424 predicted values.

425

426 In assessing the performance of the EEC prediction model given in Equation 10, the mean absolute

427 percentage error (MAPE, as defined in Equation 11) was also used:

428

$$\text{MAPE} = 100 \times \frac{1}{n} \sum \frac{\left| EEC_{obs} - EEC_{pred} \right|}{\left| EEC_{obs} \right|} \qquad (10)$$

429

430 where n is the number of data points, EEC_{obs} represent the EEC values obtained from observations and

431 EEC_{pred} represent EEC values obtained from Equation 10.

432

433 Table 4 compares the MAPEs for the EEC model over the 3 test sites at different T_Cs. Model results

434 showed very low error values over the 3 test sites with the largest errors observed within the lowest $T.I.$

435 bin (i.e. $T.I. = 0 - 10\%$). This suggests that for the sites studied, the EEC available to a particular turbine

436 could be estimated from knowledge of the turbulence intensities so long as the appropriate response time

437 of the turbine was represented by the use of an appropriate value for T_C when calculating $T.I.$ Testing the

438 validity of such a model over wider regions will require employing further sets of field measurements
439 from urban sites as they become available.
440

441 **5.   Conclusions**

442 High temporal resolution wind measurements from 3 potential urban roof-top sites have demonstrated the
443 gusty and turbulent nature of the urban wind resource and the potential advantages of utilising turbine
444 control systems which are designed to capture the energy available in these gusts. Results demonstrated
445 elevated available additional energy (high EEC) under conditions of higher $T.I.$ values, suggesting that
446 accurate modelling of turbulence intensities could inform calculations of the additional energy available if
447 optimal gust tracking solutions were found. The levels of excess energy were determined not only by
448 local roughness characteristics but also by the above roof elevation of the sites. For short mast roof-top
449 applications, gust tracking could be particularly advantageous. Available power and EEC are shown to
450 decrease with increasing averaging time (T_C) related to the response time of the VAWT, suggesting that
451 faster system response times may be essential to capture the energy within the gusts. Twice the excess
452 energy was available with a 10 s response compared to 60 s. Wind resource and energy systems
453 assessment based on turbulence intensities was shown to vary with different values of T_C illustrating the
454 importance of specifying the data resolution when quoting $T.I.$ values and properly matching T_C to the
455 expected response time of the proposed turbine. Finally, an analytical model for estimating the excess
456 energy available at a potential urban site was proposed by assessing the relationship between $T.I.$ and
457 EEC.

458
459
460
461
462
463
464
465
466
467
468
469
470
471

References

[1]   HM Government. Climate Change Act 2008. London, UK. The Stationary Office, 2008.

[2]   HM Government. Energy Act 2008. London, UK. The Stationary Office, 2008.

[3]   Baskut O, Ozgener O, Ozgener L. Second law analysis of wind turbine power plants: Cesme, Izmir example. *Energy*, 2011, **36**(5), pp.2535-2542.

[4]   Baskut O, Ozgener O, Ozgener L. Effects of meteorological variables on exergetic efficiency of wind turbine power plants. *Renewable and Sustainable Energy Reviews*, 2010, **14**(9), pp.3237-3241.

[5]   Allen SR, Hammond GP, McManus MC. Prospects for and barriers to domestic micro-generation: A United Kingdom perspective. *Applied Energy*, 2008, **85**(6), pp.528-544.

[6]   RenewableUK. Small Wind systems, UK Market Report. UK. 2010.

[7]   Britter R, Hanna S. Flow and dispersion in urban areas. *Annual Review of Fluid Mechanics*, 2003, **35**(1), pp.469-496.

[8]   McIntosh S, Babinsky H, Bertenyi T. Optimizing the Energy Output of Vertical Axis Wind Turbines for Fluctuating Wind Conditions. *In: 45th AIAA Aerospace Sciences Meeting and Exhibit*.   American Institute of Aeronautics and Astronautics, 2007.

[9]   Van der Hoven I. Power spectrum of horizontal wind speed in the frequency range from 0.0007 to 900 cycles per hour. *Journal of Meteorology*, 1957, **14**(2), pp.160-164.

[10]   Howell R, Qin N, Edwards J, Durrani N. Wind tunnel and numerical study of a small vertical axis wind turbine. *Renewable Energy*, 2010, **35**(2), pp.412-422.

[11]   Pedersen T. On wind turbine power performance measurements at inclined airflow. *Wind Energy*, 2004, **7**(3), pp.163-176.

[12]   Aslam Bhutta MM, Hayat N, Farooq AU, Ali Z, Jamil SR, Hussain Z. Vertical axis wind turbine–A review of various configurations and design techniques. *Renewable and Sustainable Energy Reviews*, 2012, **16**(4), pp.1926-1939.

[13]   Danao LA, Eboibi O, Howell R. An experimental investigation into the influence of unsteady wind on the performance of a vertical axis wind turbine. *Applied Energy*, 2013, **107**, pp.403-411.

[14]   Scelba G, Consoli A. Gust tracking capability of small direct-drive wind turbines. *In: Sustainable Energy Technologies (ICSET), 2010 IEEE International Conference*. IEEE, 2010, pp.1-6.

[15]   Acosta JL, Combe K, Djokic SZ, Hernando-Gil I. Performance assessment of micro and small-scale wind turbines in urban areas. *Systems Journal, IEEE*, 2012, **6**(1), pp.152-163.

[16]   Hanna SR, Brown MJ, Camelli FE, Chan ST, Coirier WJ, Kim S, Hansen OR, Huber AH, Reynolds RM. Detailed simulations of atmospheric flow and dispersion in downtown Manhattan: An application of five computational fluid dynamics models. *Bulletin of the American Meteorological Society*, 2006, **87**(12), pp.1713-1726.

507 [17] Wieringa J. Gust factors over open water and built-up country. *Boundary-Layer Meteorology*,
508   1973, **3**(4), pp.424-441.

509 [18] Jackson P. The evaluation of windy environments. *Building and Environment*, 1978, **13**(4),
510   pp.251-260.

511 [19] Millward-Hopkins JT, Tomlin AS, Ma L, Ingham D, Pourkashanian M. Estimating aerodynamic
512   parameters of urban-like surfaces with heterogeneous building heights. *Boundary-Layer*
513   *Meteorology*, 2011, **141**(3), pp.443-465.

514 [20] Eliasson I, Offerle B, Grimmond CSB, Lindqvist S. Wind fields and turbulence statistics in an
515   urban street canyon. *Atmospheric Environment*, 2006, **40**, pp.1-16.

516 [21] Rafailidis S. Influence of building areal density and roof shape on the wind characteristics above
517   a town. *Boundary-Layer Meteorology*, 1997, **85**(2), pp.255-271.

518 [22] Bertényi T, Wickins C, McIntosh S. Enhanced energy capture through gust-tracking in the urban
519   wind environment. *In: 48th AIAA Aerospace Sciences Meeting*, Orlando, Florida, USA. 2010.

520 [23] Shamshirband S, Petković D, Saboohi H, Anuar NB, Inayat I, Akib S, Ćojbašić Ž, Nikolić V,
521   Mat Kiah ML, Gani A. Wind turbine power coefficient estimation by soft computing
522   methodologies: comparative study. *Energy Conversion and Management*, 2014, **81**, pp.520-526.

523 [24] Abdullah M, Yatim A, Tan C, Saidur R. A review of maximum power point tracking algorithms
524   for wind energy systems. *Renewable and Sustainable Energy Reviews*, 2012, **16**(5), pp.3220-
525   3227.

526 [25] Penna P. Wind tunnel tests of the Quiet Revolution Ltd. QR5 vertical axis wind turbine. *Institute*
527   *for Aerospace Research, National Research Council Canada, Rept. LTR-AL-2008-0004*, 2008.

528 [26] Ozgener O, Ozgener L. Exergy and reliability analysis of wind turbine systems: a case study.
529   *Renewable and Sustainable Energy Reviews*, 2007, **11**(8), pp.1811-1826.

530 [27] Bertenyi T, Young T. Power electronics solutions for Vertical Axis urban wind turbines. *In:*
531   *Electrical Power & Energy Conference (EPEC)*. IEEE, 2009, pp.1-7.

532 [28] Cook NJ. Designers guide to wind loading of building structures. Part 1. 1986.

533 [29] Nakamura M, Nanayakkara N, Yoshida H, Hatazaki H. Modelling and Prediction of Effective
534   Wind speed for Wind Turbine Operations *In: Proceedings - International Conference on*
535   *Automation ICAUTO-95*, December 11-14, Indore, India. Allied Publishers Limited, 1995,
536   pp.225-228.

537 [30] Haque ME, Negnevitsky M, Muttaqi KM. A novel control strategy for a variable speed wind
538   turbine with a permanent magnet synchronous generator. *In: Industry Applications Society*
539   *Annual Meeting, 2008. IAS'08. IEEE*: IEEE, 2008, pp.1-8.

540 [31] Eriksson S, Kjellin J, Bernhoff H. Tip speed ratio control of a 200 kW VAWT with synchronous
541   generator and variable DC voltage. *Energy Science & Engineering*, 2013, **1**(3), pp.135-143.

542   [32]   Thongam J, Bouchard P, Ezzaidi H, Ouhrouche M. Wind speed sensorless maximum power point
543   tracking control of variable speed wind energy conversion systems. *In: Electric Machines and*
544   *Drives Conference, 2009. IEMDC'09. IEEE International*: IEEE, 2009, pp.1832-1837.

545   [33]   Jeong HG, Seung RH, Lee KB. An improved maximum power point tracking method for wind
546   power systems. *Energies*, 2012, **5**(5), pp.1339-1354.

547   [34]   Zhu Y, Cheng M, Hua W, Wang W. A Novel Maximum Power Point Tracking Control for
548   Permanent Magnet Direct Drive Wind Energy Conversion Systems. *Energies*, 2012, **5**(5),
549   pp.1398-1412.

550   [35]   UK   Met   Office.   UK   Climate   Summaries.   Available   from:
551   http://www.metoffice.gov.uk/climate/uk/. 2013. [Accessed August, 2013].

552   [36]   Millward-Hopkins JT, Tomlin AS, Ma L, Ingham D, Pourkashanian M. The predictability of
553   above roof wind resource in the urban roughness sublayer. *Wind Energy*, 2012, **15**(2), pp.225-
554   243.

555   [37]   Millward-Hopkins JT, Tomlin AS, Ma L, Ingham D, Pourkashanian M. Assessing the potential
556   of urban wind energy in a major UK city using an analytical model. *Renewable Energy*, 2013, **60**,
557   pp.701-710.

558   [38]   Balogun AA, Tomlin AS, Wood CR, Barlow JF, Belcher SE, Smalley RJ, Lingard JJ, Arnold SJ,
559   Dobre A, Robins AG, Martin D, Shallcross DE. In-street wind direction variability in the vicinity
560   of a busy intersection in central London. *Boundary-Layer Meteorology*, 2010, **136**(3), pp.489-
561   513.

562   [39]   IEC 61400-12-1. Wind Turbines – Part 12-1 : Power performance measurement of Electricity
563   producing wind turbines. Ed, 2005.

564   [40]   Hedevang E. Wind turbine power curves incorporating turbulence intensity. *Wind Energy*, 2014,
565   **17**(2), pp.173-195.

566   [41]   Allen S, Hammond G, McManus M. Energy analysis and environmental life cycle assessment of
567   a micro-wind turbine. *Proceedings of the Institution of Mechanical Engineers, Part A: Journal of*
568   *Power and Energy*, 2008, **222**(7), pp.669-684.

569   [42]   Abohela IMMM. Effect of roof shape, wind direction, building height and urban configuration on
570   the energy yield and positioning of roof mounted wind turbines. 2012.

571   [43]   Ledo L, Kosasih P, Cooper P. Roof mounting site analysis for micro-wind turbines. *Renewable*
572   *Energy*, 2011, **36**(5), pp.1379-1391.

573   [44]   Kaiser K, Langreder W, Hohlen H, Hojstrup J. Turbulence Correction of Power Curve. *In: Wind*
574   *Energy: Proceedings of the Euromech Colloquium*. Peinke J, Schaumann P and Barth S, eds.
575   New York: Springer, 2007, pp.159-162.

576   [45]   Petersen EL, Mortensen NG, Landberg L, Højstrup J, Frank HP. Wind power meteorology. Part

577   I: Climate and turbulence. *Wind Energy*, 1998, **1**(s 1), pp.25-45.

578   [46]   Kooiman S, Tullis S. Response of a vertical axis wind turbine to time varying wind conditions

579   found within the urban environment. *Wind Engineering*, 2005, **34**(4), pp.389-401.

580

581

582

583

584

585

586

587

588

589

590

591

592

593

594

595

596

597

598

599

600

601

602

Figure Legends

603

604 **Figure 1**: Frequency distribution of fluctuating wind energy within the internal sub-layer, adapted from Van Der
605 Hover [9]

606 **Figure 2**: Real world measured urban wind resource at a Manchester roof-top site illustrating a period with high
607 fluctuations of the urban wind resource; the 1Hz data (dotted lines) and 0.1Hz data (solid lines).

608 **Figure 3**: Power coefficient for a QR5 VAWT model as a function of non-dimensional tip speed ratio, measured
609 under a full-scale wind tunnel test by Quiet Revolution highlighting the maximum power coefficient (C_{pmax}) and
610 maximum tip speed ratio (λ_{max}) (Adapted from [25]).

611 **Figure 4**: Average monthly power (top), $T.I.$ (middle) and mean wind speed (bottom) values at the two sites for a
612 one year data at a sampling frequency of 1 s (solid lines) and an averaging time of 10 mins (dotted lines).

613 **Figure 5**: A comparison of the average power curve to power curves sorted by bands of $T.I.$ for one year dataset
614 parsed at 10 min bursts at (a) Unileeds (H1), (b) Unileeds(H2) and (c) Manchester sites.

615 **Figure 6**: The $T.I.$ distribution for a one year at both sites analysed, for which the power curves are plotted in Figure
616 5 at T_C = 1 s.

617 **Figure 7**: Plot showing the average monthly EEC values at the two sites across the year at T_C = 1 s.

618 **Figure 8**: EEC at T_C = 1 s for a one year wind input at both sites (Unileeds (H1 and H2) and Manchester). Each
619 point represents 10 min bursts, illustrating the expected potential contribution of gust tracking within both sites.

620 **Figure 9**: Effect of change in T_C on average EEC (left) and wind power (right) at Unileeds and Manchester
621 highlighting power and energy gain with decreasing averaging time.

622 **Figure 10:** The relationship between average power, EEC and $T.I.$ with averaging time for a year at the
623 Manchester site demonstrated.

624 **Figure 11:** The relationship between EEC and $T.I.$ with averaging time at both sites

625

626

627

628

629

630

631

632

Sites	T.I. Bins				$P_{1s} - P_{10mins}$
	10 - 20%	**20 - 30%**	**30 - 40%**	**40 - 50%**	
Unileeds(H1)	6.97	25.77	34.13	51.73	29.79
Unileeds(H2)	8.04	18.64	32.36	60.01	33.63
Manchester	16.57	25.63	28.54	49.55	28.83

Table 1: Percentage increase across the turbulence intensity bins from the Average Power (P_{10mins}) calculated from mean wind speed at 10 mins (as shown in the power plots in Figure 5)

SITE DESCRIPTION	EEC (%)	z_o (m)
Coastal site	3.3	0.005
Open country	16.1	0.05
Semi Urban	22.7	0.2
Urban	> 23	> 0.7
Unileeds (H1)	35.3	1
Unileeds (H2)	50	1
Manchester	53.4	0.9

Table 2: A summary of the *EEC* from some analysed turbine sites with their relative roughness heights (adapted from [22]) and urban sites selected in this paper.

SITES	TURBINE CONFIGURATIONS	
	Tb1	**Tb2**
Unileeds (H1)	6.93 %	17.85%
Unileeds (H2)	10.68%	23.21 %
Manchester	8.21 %	17.78%

Table 3: Summary of percentage loss in power deduced from Tb1 and Tb2 operation from assumed maximum operating frequency of 1Hz at both sites for a year

T_C	Sites		MAPE for the different $T.I.$ Bins (%)							
		$T.I.$ ranges	0-10	10-20	20-30	30-40	40-50	50-60	60-70	70-80
1s	Unileeds(H1)		8.740	1.035	2.634	0.866	1.447	1.196	0.261	1.611
	Unileeds(H2)		9.780	1.580	2.976	1.499	0.089	0.402	2.641	5.456
	Manchester		11.500	1.485	1.643	3.871	4.831	4.132	1.944	1.506
10s	Unileeds(H1)		8.719	1.429	2.803	1.386	0.349	0.354	1.006	2.507
	Unileeds(H2)		8.796	1.742	3.170	2.373	2.491	3.295	4.129	1.025
	Manchester		9.444	0.251	0.374	0.785	1.177	0.057	0.528	4.419
60s	Unileeds(H1)		8.141	1.626	2.863	2.141	0.835	0.083	3.854	1.777
	Unileeds(H2)		8.366	1.757	3.271	3.151	2.320	2.038	2.245	3.547
	Manchester		8.354	1.195	1.841	0.921	0.336	0.396	1.337	2.734

Table 4: Mean absolute percentage errors (%) compared over 3 test sites at different T_C using the EEC analytical model.

Figure 1. Francis Emejeamara
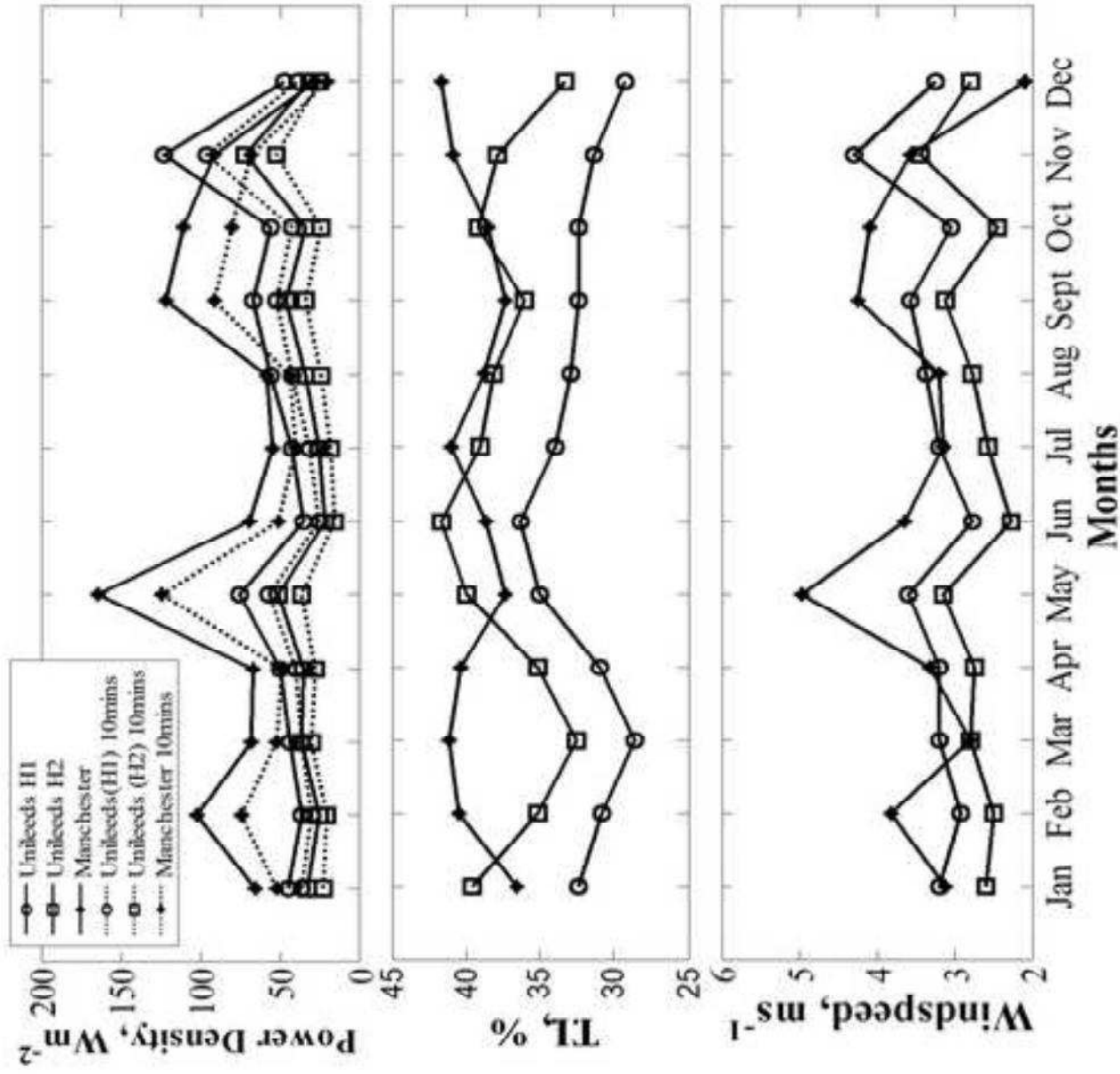
Figure 2. Francis Emejeamara
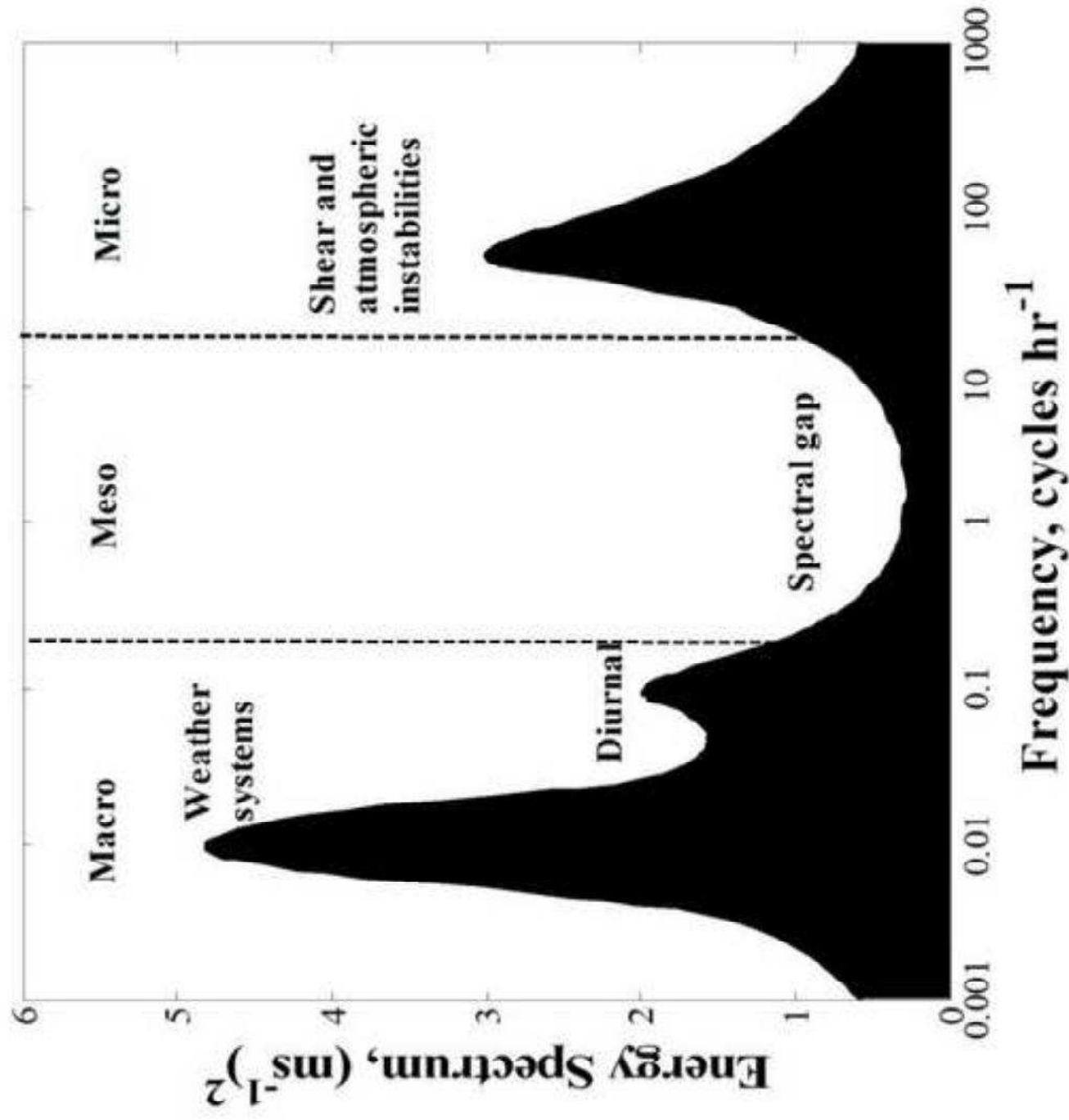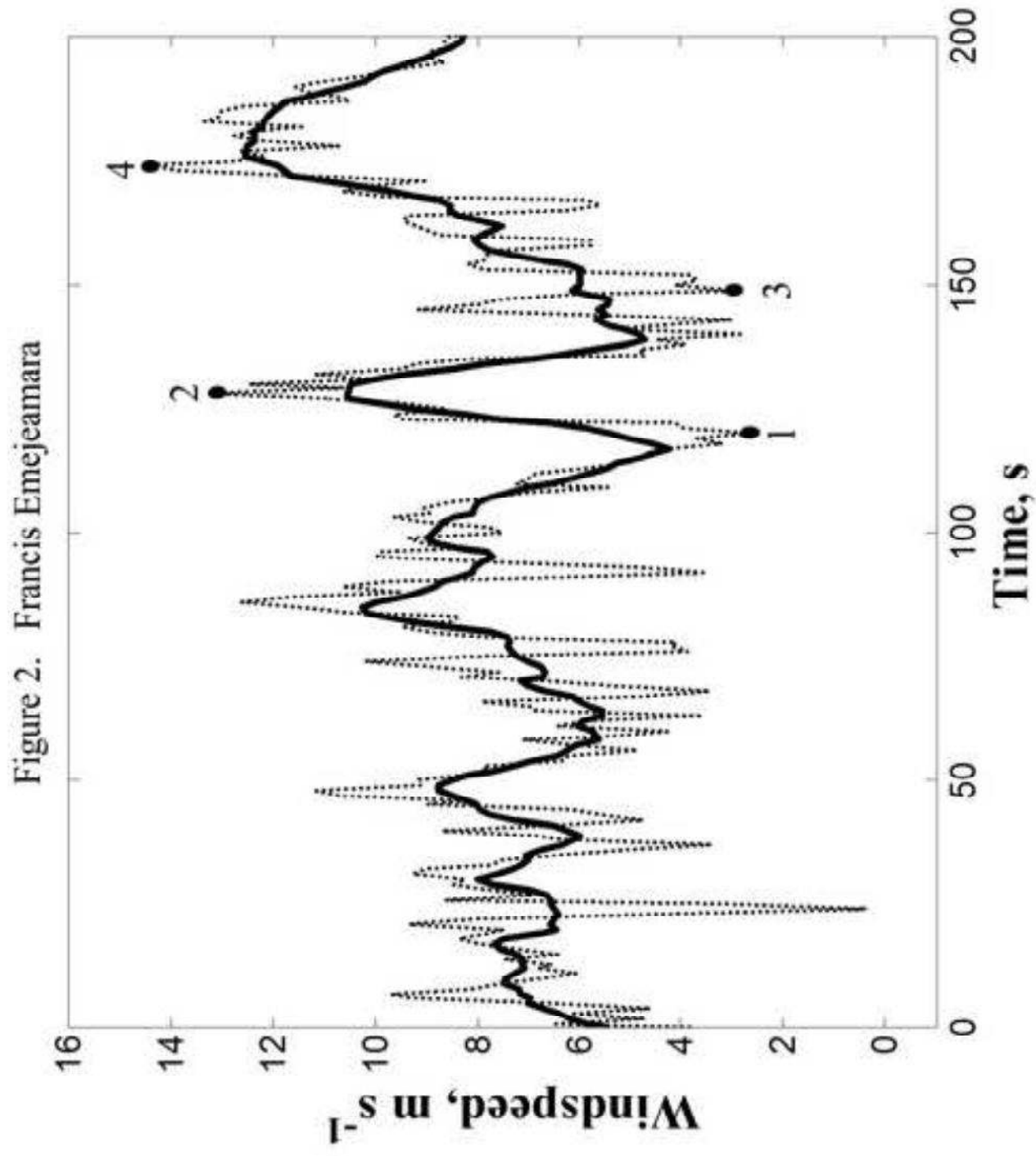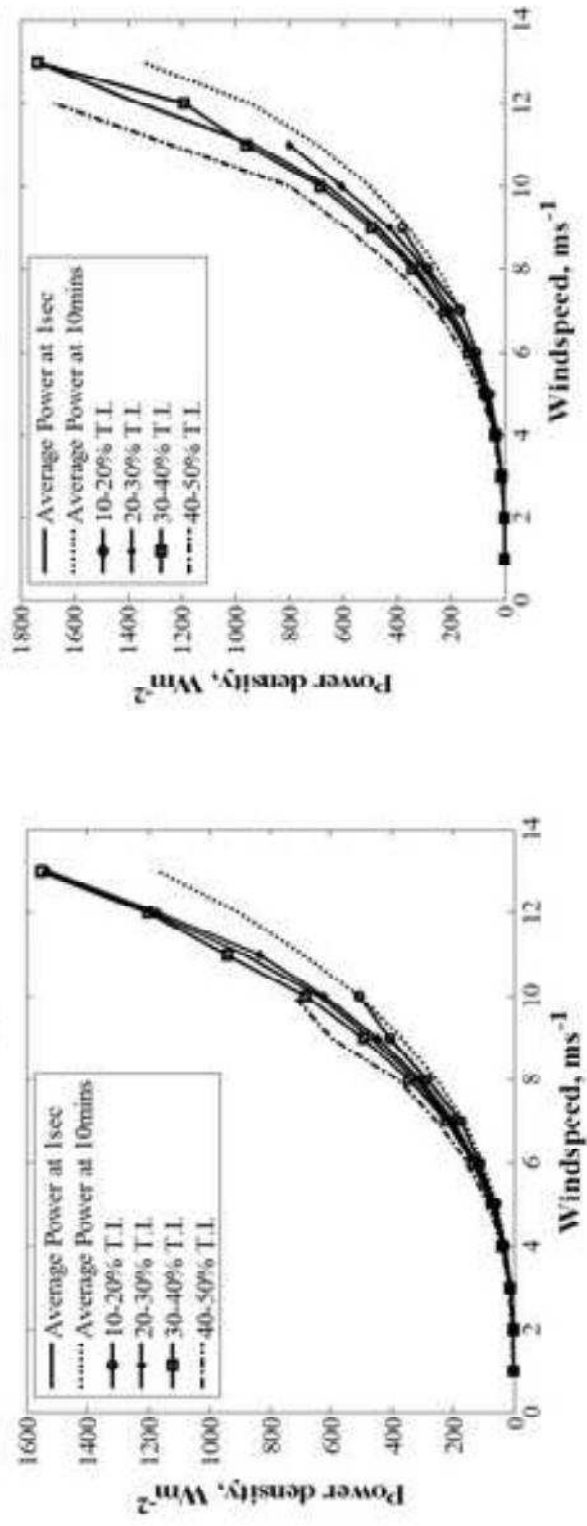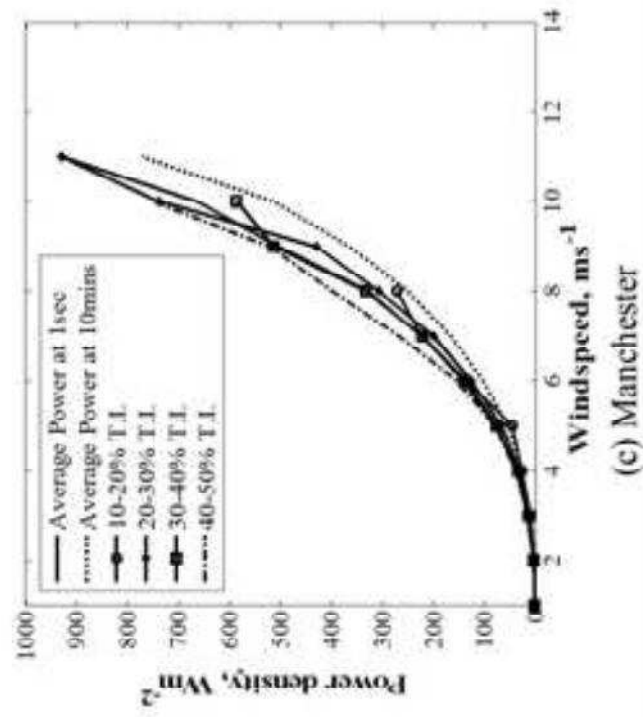
Figure 3. Francis Emejeamara
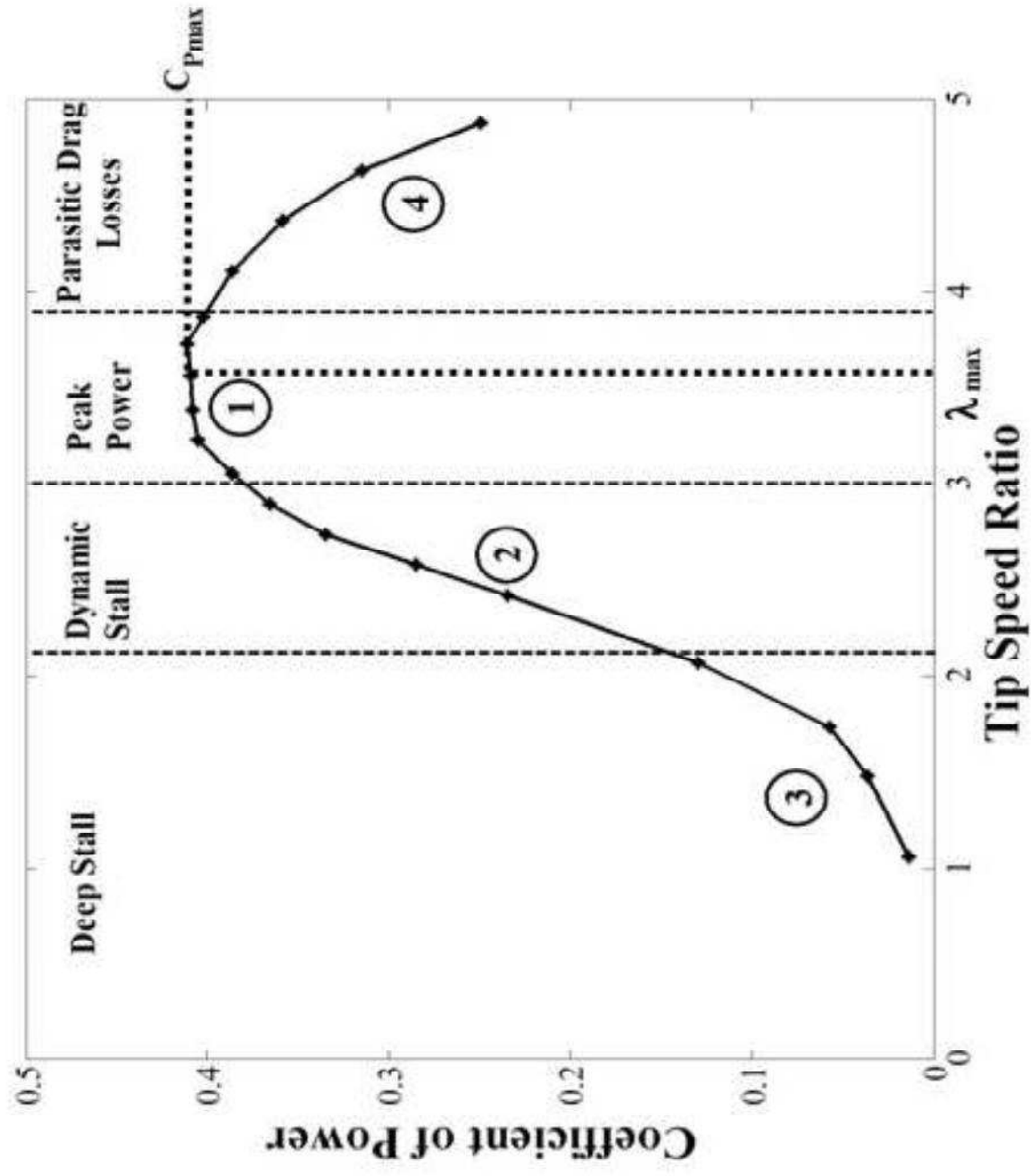
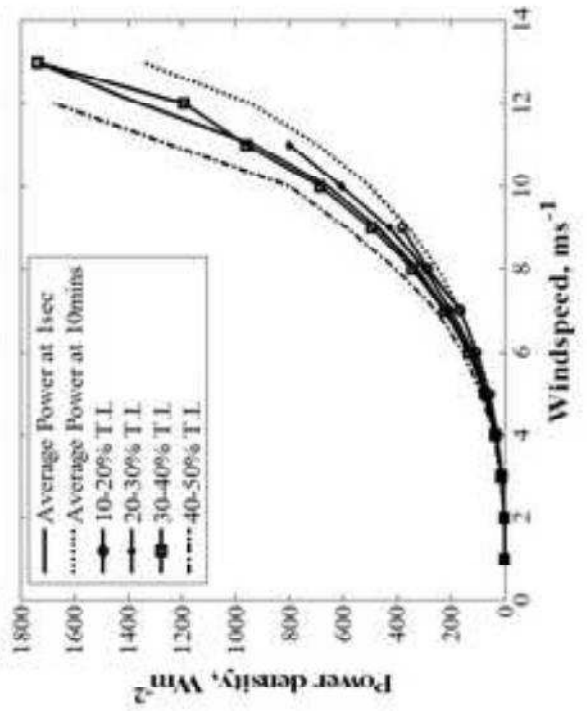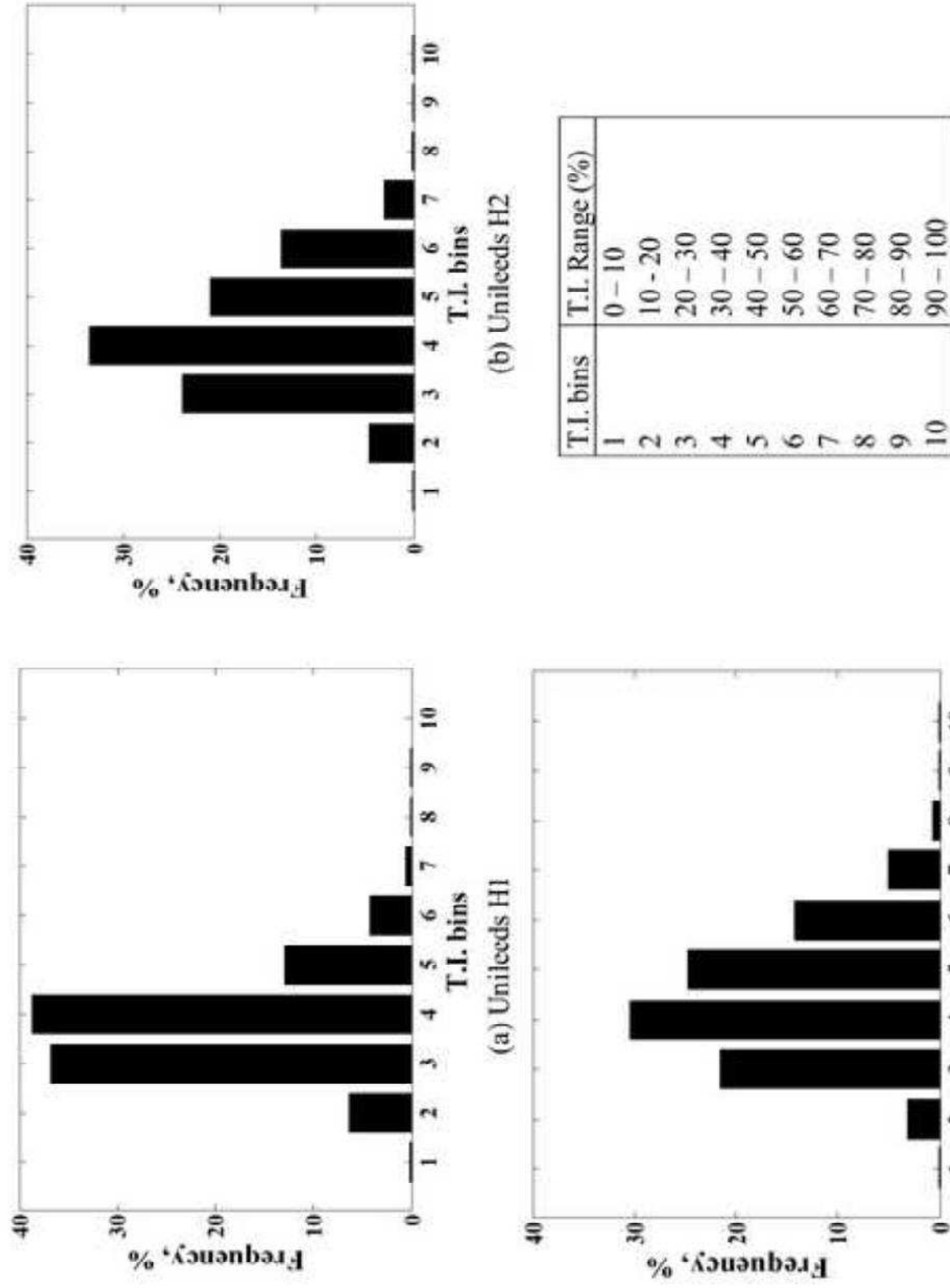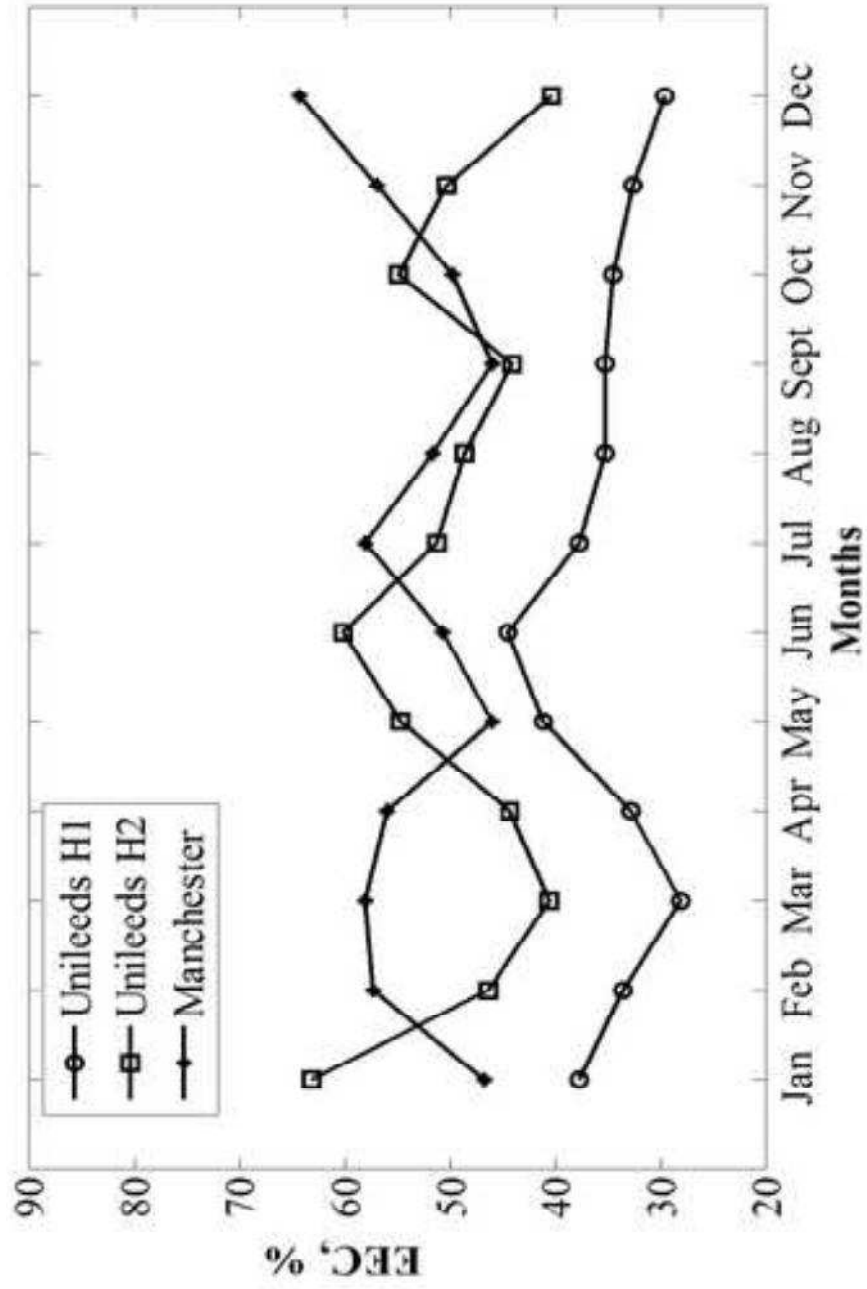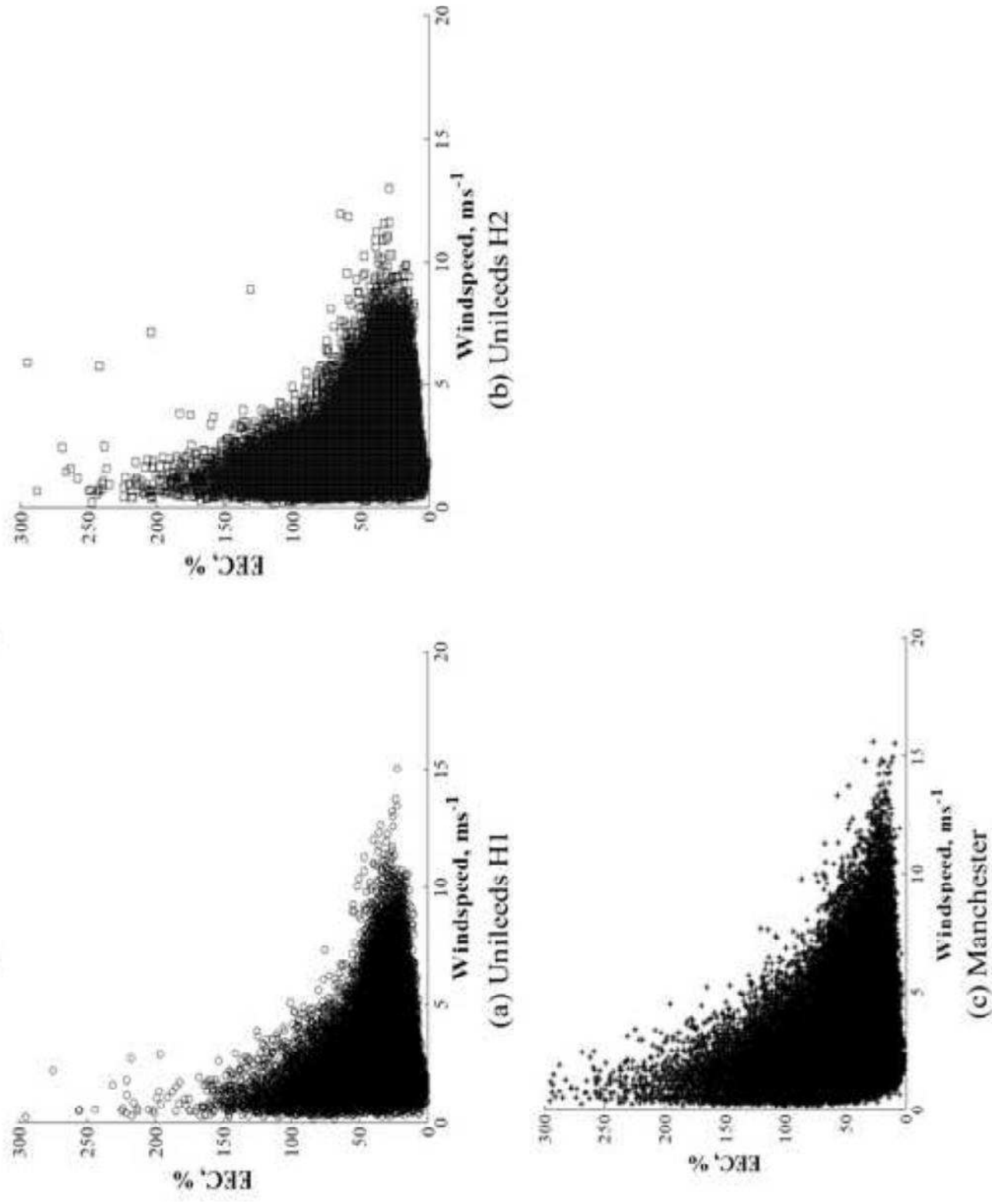Figure 4. Francis Emejeamara

Figure 5. Francis Emejeamara

(a) Unileeds H1

(b) Unileeds H2

(c) Manchester

Figure 6. Francis Emejeamara

(a) Unileeds H1

(b) Unileeds H2

(c) Manchester

T.I. bins	T.I. Range (%)
1	0 − 10
2	10 - 20
3	20 − 30
4	30 − 40
5	40 − 50
6	50 − 60
7	60 − 70
8	70 − 80
9	80 − 90
10	90 − 100

Figure 7. Francis Emejeamara

Figure 8. Francis Emejeamara

(a) Unileeds H1
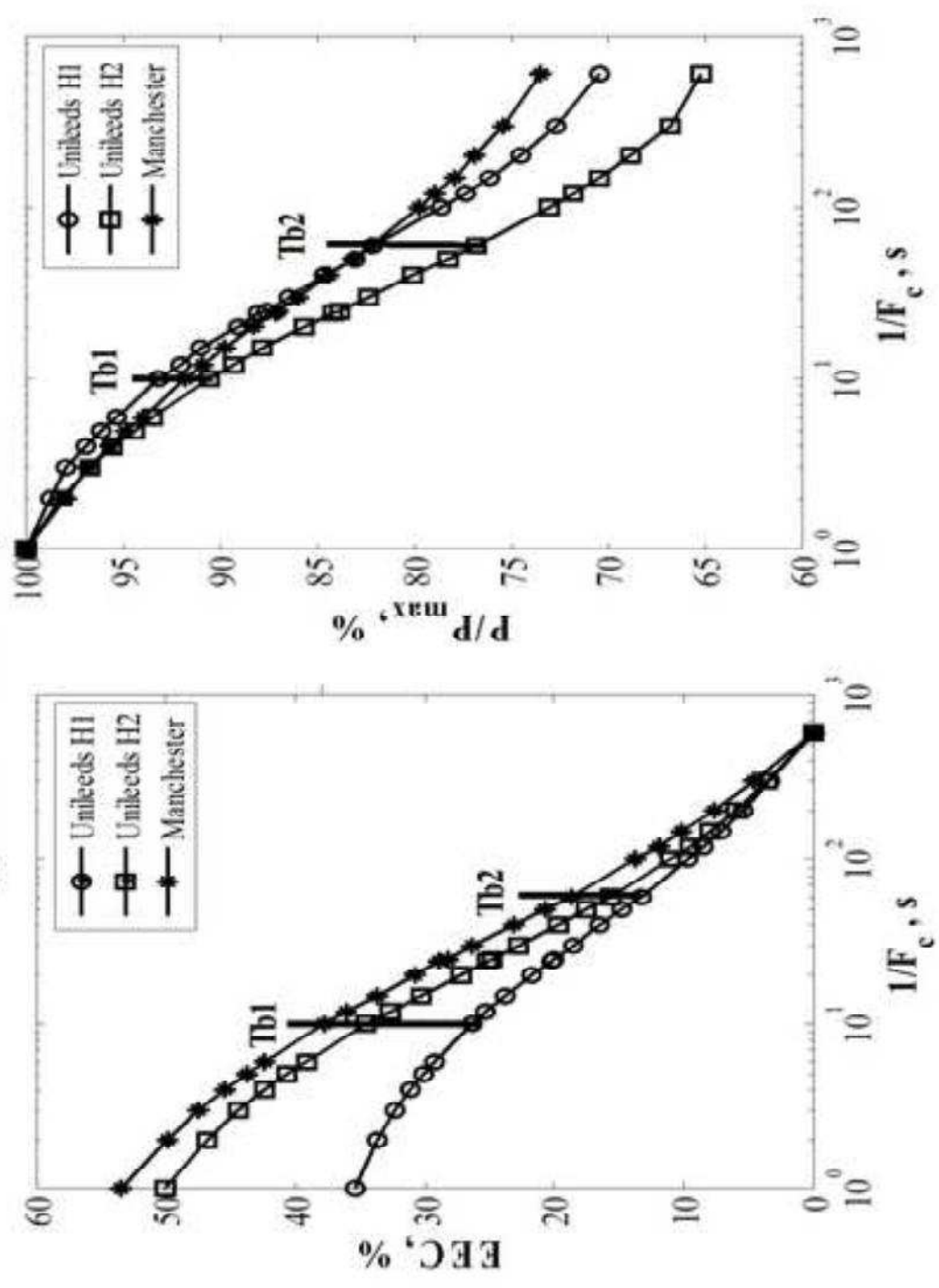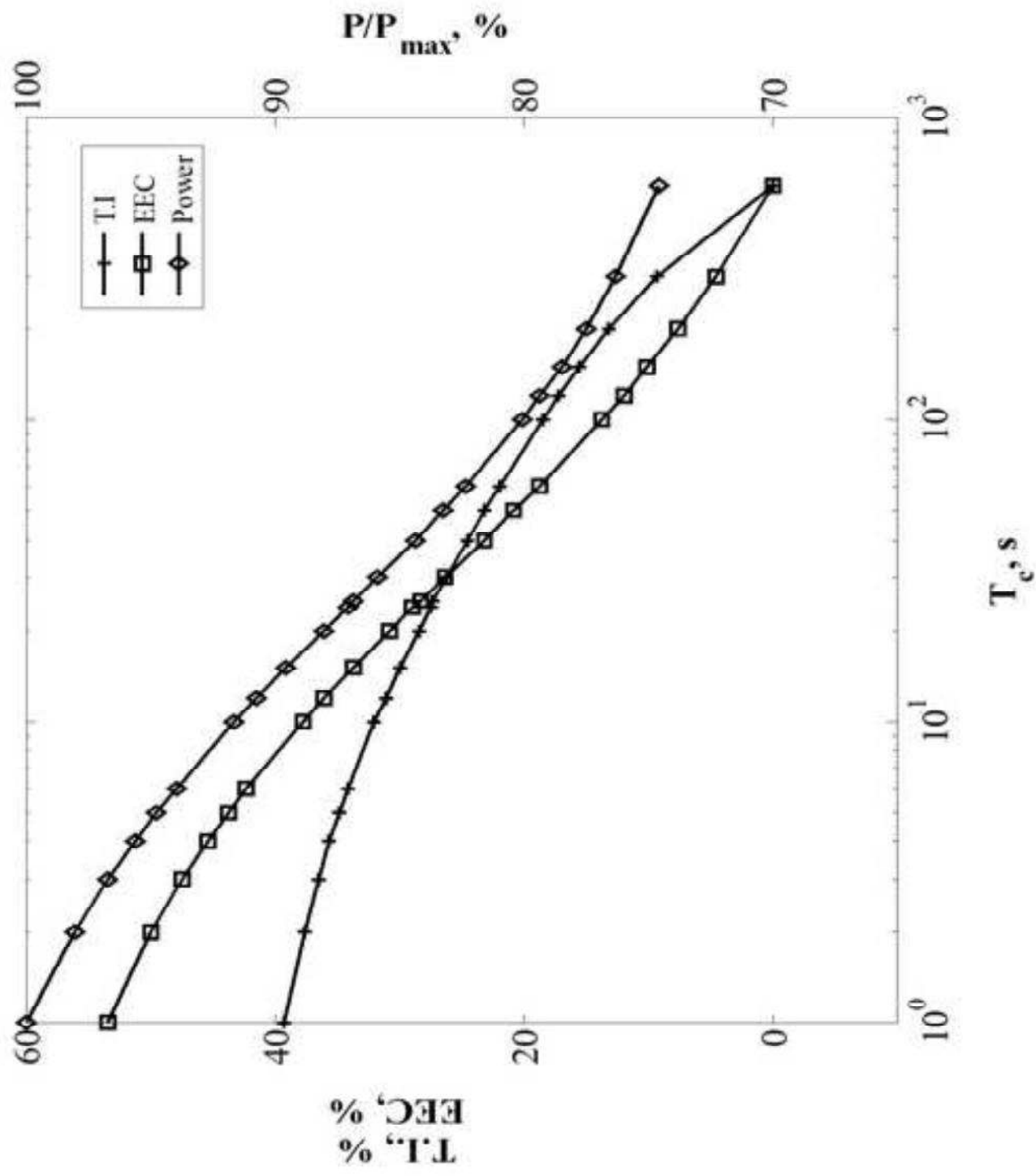
(b) Unileeds H2

(c) Manchester

Figure 9. Francis Emejeamara

Figure 10. Francis Emejeamara

Figure 11. Francis Emejeamara